

Intrinsic detection efficiency of superconducting single photon detector in the modified hot spot model

A.N. Zotova^{1,2*} and D.Yu. Vodolazov^{1,2},

¹ *Institute for Physics of Microstructures, Russian Academy of Sciences, 603950, Nizhny Novgorod, GSP-105, Russia*

² *Lobachevsky State University of Nizhni Novgorod,
23 Gagarin Avenue, 603950 Nizhni Novgorod, Russia*

We theoretically study the dependence of the intrinsic detection efficiency (IDE) of superconducting single photon detector on the applied current I and magnetic field H . We find that the current, at which the resistive state appears in the superconducting film, depends on the position of the hot spot (region with suppressed superconductivity around the place where the photon has been absorbed) with respect to the edges of the film. It provides inevitable smooth dependence IDE(I) when IDE $\sim 0.05 - 1$ even for homogenous straight superconducting film and in the absence of fluctuations. When IDE $\lesssim 0.05$ much sharper current dependence comes from the fluctuation assisted vortex entry to the hot spot located near the edge of the film. We find that weak magnetic field strongly affects IDE when the photon detection is connected with fluctuation assisted vortex entry (IDE $\ll 1$) and it weakly affects IDE when the photon detection is connected with the current induced vortex entry to the hot spot or nucleation of the vortex-antivortex pair inside the hot spot (IDE $\sim 0.05 - 1$).

PACS numbers:

I. INTRODUCTION

At the moment there are several phenomenological models which try to describe the detection mechanism of superconducting single photon detectors - SSPD (for their comparison see for example Ref. [1]). In this paper we study how one of the main characteristic of SSPD - intrinsic detection efficiency (IDE) depends on the current and magnetic field in the modified hot spot model, which takes into account both the nonuniform current distribution around the hot spot (current crowding effect [8]) and suppression of the superconductivity by the current [2]. In comparison with the system detection efficiency, which defines the probability to detect the photon by the whole detector, IDE has a meaning of probability to detect the photon when it is absorbed by the main element of SSPD - superconducting current-carrying film in the form of meander [3].

The used modified hot spot model has two main qualitative differences with previous hot spot models [4–7]: we solve the current continuity equation $\text{div} j = 0$ in the film with the hot spot (which automatically gives us the maximal value of the current density near the hot spot even if it is located far from the edges of the film) and we take into account the back effect of the current redistribution on the superconducting order parameter in the film with hot spot (which gives us nucleation of the vortex-antivortex pair inside the hot spot located far from the edges of the film). The used phenomenological model of the hot spot cannot relate quantitatively the energy of the photon with the size of the hot spot and how strong the superconductivity is suppressed inside it. But we

demonstrate that the radius of the hot spot and level of suppression of superconductivity affect the photon detection mechanism and dependencies IDE(I) and IDE(H) only quantitatively.

When the hot spot (region with partially or completely suppressed superconductivity) appears in the superconducting film after photon absorption the superconducting current avoids that region and it 'crowds' near the hot spot. The current crowding effect in thin superconducting films with geometric inhomogeneities attracted large attention last years both from theoretical [8, 9] and experimental [10–13] points of view. In Ref. [8] among different problems there was considered the superconducting semi-infinite film with the edge defect in the form of the semicircle (semicircular notch - see Fig. 18 in Ref. [8]). This problem is mathematically equivalent to the infinite film with a circular notch and when the diameter of the notch $D = 2R$ is much larger than the coherence length the critical current is equal to the half of the depairing current (see Fig. 19(b) in Ref. [8]) which is consequence of the current crowding near the notch. This result coincides with our result for the finite width film with the normal spot (see Eq. (12) in Ref. [2] in the limit $\gamma \rightarrow 0$) when $w \gg 2R$, i.e. when the film becomes formally 'infinite'. Finite width of the film changes this universal result and besides the critical current depends now on the position of the normal spot (or notch) with respect to the edges of the film.

In our previous work [2] we consider two locations of the hot spot: in the center and at the edge of the film. We find that in these two limiting cases the resistive state starts (in absence of fluctuations) at different critical currents, which were called as a detection currents I_{det} , via appearance of the current induced vortices and their motion across the film. We stress here that vortex nucleation is *the direct consequence* of the spatially nonuniform dis-

*Electronic address: vodolazov@ipmras.ru

tribution of the superconducting order parameter and supercurrent in the superconducting film with the hot spot.

In this work we find I_{det} at different locations of the hot spot in the film. We show that I_{det} reaches the minimal value I_{det}^{min} when the hot spot is located near the edge of the film and it has maximal value when the hot spot is located in the center of the film. We also calculate the energy barrier for the vortex entry to the superconducting film with the hot spot when $I < I_{det}^{min}$ and find the rate of fluctuation assisted vortex entry as function of the current. These results allow us to calculate dependence IDE(I) in wide range of the currents and we argue that vortices play important role both when $IDE \simeq 1$ and when $IDE \ll 1$. Application of the magnetic field decreases locally the current density in one half of the film and increases it in another half because of field induced screening currents. We show that in the used model it leads to strong increase of IDE when the photon detection is governed by the fluctuation assisted vortex entry to the film ($IDE \ll 1$) and the effect becomes much weaker when the photon detection is determined by the current induced vortex entry ($IDE \sim 0.1 - 1$).

II. MODEL

In our hot spot model (as in other hot spot models [4–7]) it is assumed that in the place, where the photon is absorbed, there is nonequilibrium (‘heated’) distribution of the quasiparticles over the energy which locally suppresses the superconductivity and it leads to redistribution of the current density in the film. Calculation of actual nonequilibrium distribution function of quasiparticles f_{neq} needs solution of the kinetic equation and it is very complicated problem [14] and we do not study it in this work. Our aim is to study how the presence of the region with locally suppressed superconductivity (superconducting order parameter) affects the value of the critical current, at which the superconducting state of the film with hot spot (HS) becomes unstable. For this purpose we numerically solve the Ginzburg-Landau equation for the superconducting order parameter

$$\xi_{GL}^2 \left(\nabla - i \frac{2e}{\hbar c} A \right)^2 \Delta + \left(1 - \frac{T_{bath}}{T_c} + \Phi_1 - \frac{|\Delta|^2}{\Delta_{GL}^2} \right) \Delta = 0 \quad (1)$$

with the additional term

$$\Phi_1 = \int_{|\Delta|}^{\infty} \frac{2(f^0 - f)}{\sqrt{\epsilon^2 - |\Delta|^2}} d\epsilon, \quad (2)$$

which takes into account the impact of nonequilibrium quasiparticle distribution function $f(\epsilon) \neq f^0(\epsilon) = 1/(\exp(\epsilon/k_B T_{bath}) + 1)$. In Eq. (1) A is a vector potential, $\xi_{GL}^2 = \pi \hbar D / 8 k_B T_c$ and $\Delta_{GL}^2 = 8 \pi^2 (k_B T_c)^2 / 7 \zeta(3) \simeq 9.36 (k_B T_c)^2$ are the zero temperature Ginzburg-Landau coherence length and the order parameter correspondingly. Together with Eq. (1) we also solve continuity

equation $div j_s = 0$ (j_s is a superconducting current density) to find the distribution of the current density.

In numerical calculations it is convenient to use dimensionless units. Therefore we scale the length in units $\xi(T_{bath}) = \xi_{GL} / (1 - T_{bath}/T_c)^{1/2}$, Δ in units $\Delta_{eq} = \Delta_{GL} (1 - T_{bath}/T_c)^{1/2}$ and A in units $\Phi_0 / 2\pi \xi$ (Φ_0 is a magnetic flux quantum). In these units Eq. (1) has a following form

$$(\nabla - i \tilde{A})^2 \tilde{\Delta} + (\alpha - |\tilde{\Delta}|^2) \tilde{\Delta} = 0, \quad (3)$$

where $\alpha = (1 - T_{bath}/T_c + \Phi_1) / (1 - T_{bath}/T_c)$.

In Eq. (3) the effect of absorbed photon on the superconducting properties of the film is described by the parameter α (in equilibrium $\alpha = 1$) which is determined by $f(\epsilon)$. In our model we put $\alpha = const < 1$ inside the hot spot region which leads to local suppression of $|\Delta|$ not only inside but also outside the hot spot (due to proximity effect). Surely this assumption oversimplifies the real situation where α depends on the coordinate and we cannot expect that our results are *quantitatively* valid. But below we demonstrate that *qualitatively* the obtained results does not depend on actual value of α (which governs the suppression of $|\Delta|$ inside HS) and we expect that they are valid in the real situation with coordinate dependent $\alpha(r)$.

To have an insight on the possible values of α one can use the local temperature approach which implies that $f(\epsilon)$ can be described by the Fermi-Dirac function with the local temperature T_{loc} which is different from the bath temperature T_{bath} . It is easy to show (with help of Eq. (3)) that in this limit

$$\alpha(\vec{r}, t) = (1 - T_{loc}(\vec{r}, t)/T_c) / (1 - T_{bath}/T_c) \quad (4)$$

The area where $T_{loc} > T_{bath}$ increases in time due to diffusion of hot quasiparticles from the place where the photon was absorbed. From Eq. (3) it follows that the order parameter is suppressed stronger in the place where $T_{loc} > T_c$ and $\alpha < 0$. At some moment in time the region where $T_{loc} > T_c$ reaches the maximal size and it is naturally to model the hot spot by the circle with radius R and put $\alpha = 0$ inside the circle. In this case the radius of the spot R and energy of the absorbed photon ch/λ are roughly related as

$$\eta \frac{ch}{\lambda} \simeq d \pi R^2 \frac{H_{cm}^2}{8\pi} \quad (5)$$

where $H_{cm} = \Phi_0 / 2\sqrt{2}\pi \xi \lambda_L^2$ is the thermodynamic magnetic field, λ_L is the London penetration depth, d is the thickness of the film and $H_{cm}^2 / 8\pi$ is the superconducting condensation energy per unit of volume. Coefficient $0 < \eta < 1$ takes into account that only part of the energy of the photon is delivered for suppression of Δ and the rest of the photon’s energy goes for heating of quasiparticles and phonons.

When the photon is absorbed at the edge of the film the nonequilibrium quasiparticles cannot leave the sample and we model the hot spot by the semicircle with

larger radius $R' = \sqrt{2}R$ to keep the area of the hot spot unchanged.

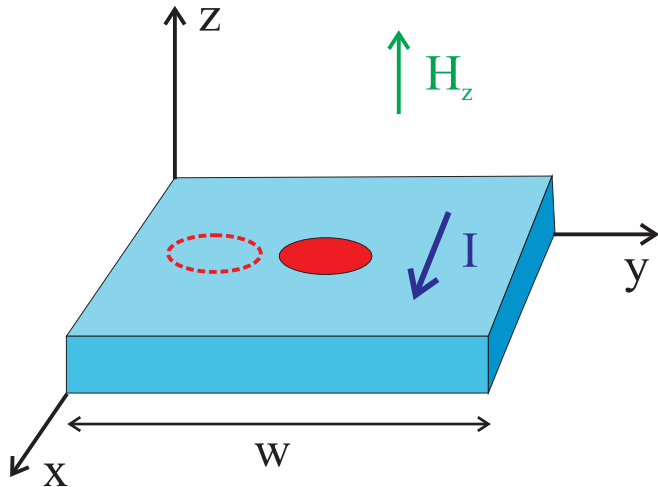


FIG. 1: Model geometry: two-dimensional film with width w and transport current I placed in perpendicular magnetic field. The hot spot is modelled by the finite size region where $\alpha < 1$ (it models the heating of quasiparticles in this region due to absorbed photon).

From Eq. (3) it follows that for the spots with $R \gg \xi$ the order parameter inside the hot spot is $\simeq \sqrt{\alpha}\Delta_{eq}$ when $\alpha \geq 0$, and it is equal to zero when $\alpha < 0$. Remind here that different α corresponds to different level of the nonequilibrium inside the hot spot (in the local temperature approximation this relation is given by Eq. (4)). Due to proximity effect the order parameter is suppressed partially also at $r > R$ and it becomes larger than $\sqrt{\alpha}\Delta_{eq}$ inside the hot spot when the radius is about of the coherence length.

In numerical calculations we consider the film of finite width w and length $L = 4w$ with different locations of the hot spot (region where $\alpha < 1$) across the film - see Fig.1. We also add to the right hand side of Eq. (3) the term with time derivative $\partial\tilde{\Delta}/\partial t$ which allows us to find not only the value of the critical current (above this current there is no stationary solution of Eq. (3)) but also the place in the film where vortices nucleate.

III. DETECTION CURRENT

Let us now to discuss what is the mechanism of destruction of the superconducting state in the superconducting film with the photon induced hot spot. We find that when the hot spot is located at the edge of the film and the current exceeds the critical value I_{pass} the vortex enters the hot spot via edge of the film and than it passes through the film (see the sketch in the Fig. 2(a)). In Ref. [2], in the local temperature approach, we find that the vortex motion may strongly heat the superconductor and it leads to the appearance of the normal domain. In the

following we assume that passage of even single vortex through the film is a sufficient condition for destruction of the superconducting state in the superconductor biased at the current, not much smaller than the depairing current.

We also find that for relatively large radius of the hot spot ($R \gtrsim 3\xi$ when $\alpha = 0$) at currents $I_{en} < I < I_{pass}$ the vortex enters the hot spot, but it cannot leave it (the similar effect was found earlier in Ref. [15] at study of the effect of edge defects on the vortex penetration to the superconducting film). The hot spot, as a region with suppressed superconductivity, could be considered as a photon induced pinning center and vortex becomes unpinning only at the current $I \geq I_{pass}$. But in contrast with the usual pinning center the hot spot exists only during short period of time $\min(\tau_{e-ph}, \tau_{e-e})$, where τ_{e-ph} and τ_{e-e} are the inelastic relaxation times due to electron-phonon or electron-electron interaction, respectively. Indeed, the nonequilibrium quasiparticles with energy $\epsilon < \Delta_{eq}$ cannot diffuse out the hot spot and they relax to equilibrium via (whatever is stronger) electron-phonon or electron-electron interaction with quasiparticles having energy $\epsilon > \Delta_{eq}$ and which can diffuse away from the region with suppressed $|\Delta|$.

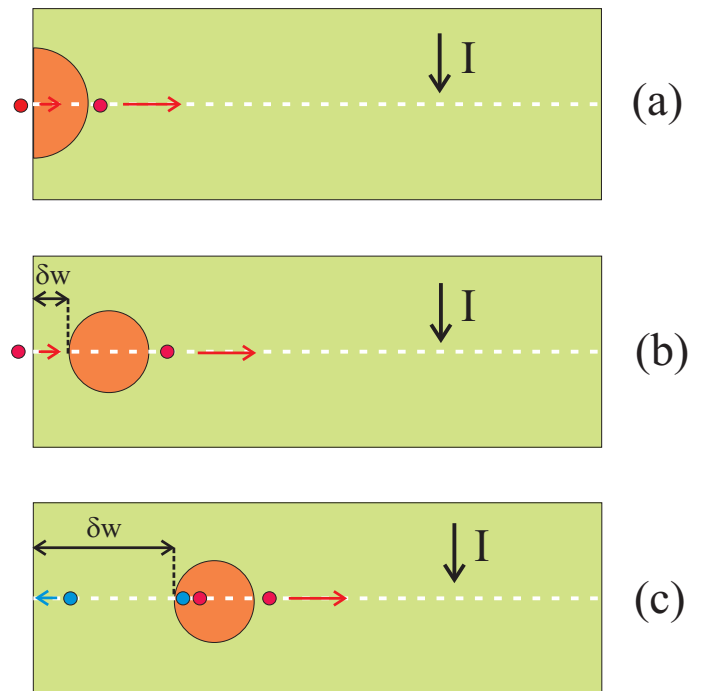


FIG. 2: Schematic representation of mechanisms of destruction of the superconducting state at different locations of the hot spot: (a) the hot spot in the form of semicircle is located at the edge of the film, (b) the hot spot is located close to the edge of the film ($\delta w \lesssim 2\xi$), (c) the hot spot is located at distance $\delta w \gtrsim 2\xi$. In cases (a,b) the vortex enters via the nearest edge of the film, while in the case (c) the vortex/antivortex pair is nucleated inside the hot spot.

Therefore, in the range of the currents $I_{en} < I < I_{pass}$

the vortex is temporarily pinned and after 'dissociation' of the hot spot it becomes unpinned and can pass through the film or exit via the nearest edge due to interaction with its 'image' outside the film. Our numerical simulations with help of time dependent Ginzburg-Landau equation and time dependent $\alpha(t)$ confirm both scenario. Starting from the hot spot state with $\alpha = 0$ and pinned vortex we gradually increase α in time up to its equilibrium value $\alpha = 1$ (no hot spot state). We find that when the current is just above I_{en} the vortex exit via the nearest edge, while at relatively larger currents (less than I_{pass}) vortex goes through the film.

When the spot is located near the edge of the film (see Fig. 2(b)) there are the same characteristic currents I_{en} and I_{pass} - first one corresponds to the vortex entrance to the hot spot and the second one to its unpinning and the free passage of the vortex through the film. In contrast with the case drawn in Fig. 2(a), when the hot spot 'dissociates' the vortex passes the film in the whole current interval $I_{en} < I < I_{pass}$. We explain it by the larger distance from the nearest edge and smaller attraction force from the 'image' of the vortex.

When the distance (δw in Fig. 2(b,c)) between the 'edge' of hot spot and the edge of the film exceeds $\sim 2\xi$ the vortex/antivortex pair is nucleated *inside* the hot spot at the current I_{pair} . Again, if $R \gtrsim 3\xi$ vortex and antivortex becomes unpinned at larger current $I_{pass} > I_{pair}$. For such a location the 'dissociation' of the hot spot leads to the annihilation of the vortex-antivortex pair and their passage through the film occurs only at $I \geq I_{pass}$.

We find that with increasing the radius of the hot spot the gap between currents I_{en} (or I_{pair}) and I_{pass} increases. For spots with $R \lesssim 3\xi$ and $\alpha = 0$ these two currents coincide (which is connected with relatively large value of $|\Delta|$ inside the spot and worse ability to pin the vortices). The obtained results are rather general and depend on the specific value of α and width of the film only quantitatively.

The physical origin for the found results is following. Due to the current crowding effect the current density reaches maximal value near the hot spot (see Fig. 3(b)). But simultaneously there is an enlargement of the supervelocity $v_s \sim j_s/|\Delta|^2$ in or around the hot spot (see Fig. 3(c)). The last effect is crucial for stability of the superconductivity because the superconducting state becomes unstable when the velocity of superconducting electrons exceeds some critical value [15] (which is similar to the instability criteria for flowing superfluid helium). In the system with the uniform distribution of the order parameter and current density it coincides with the condition that the current density reaches the depairing current density j_{dep} . But inside and around the hot spot there is a gradient of both $|\Delta|$ and j (see Figs. 3(a,b)), these two criteria do not coincide and the vortices nucleate in the place where the supervelocity reaches the maximal value. Note, that quantitatively both these criteria are not too far from each other, because when the vortex enters the

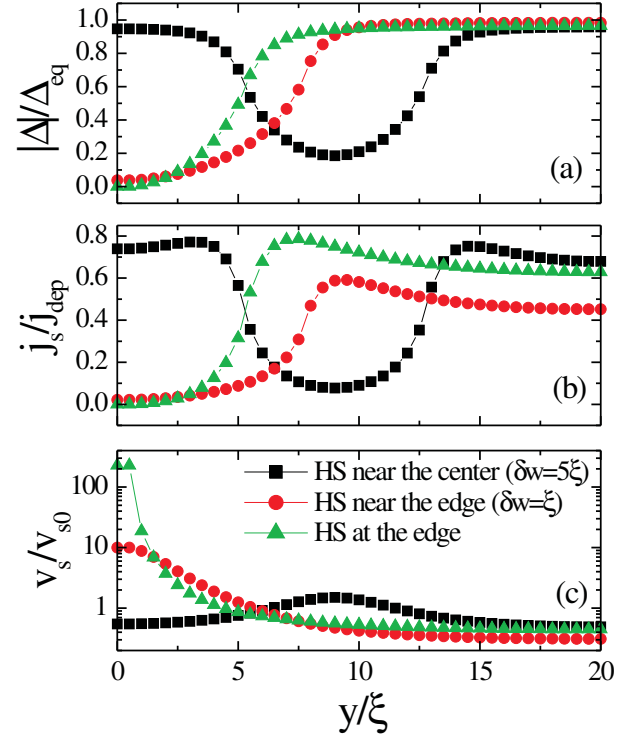


FIG. 3: Distribution of the order parameter (a), current density (b) and supervelocity (c) across the film (along the dashed lines shown in the Figs. 2(a-c)) with different locations of the hot spot. The applied current is just below I_{en} (or I_{pair}).

hot spot (or the vortex/antivortex pair is nucleated inside the hot spot) the maximal current density near the spot is close to j_{dep} (see Fig. 3(b)).

With above findings we define the photon detection current I_{det} as a current at which at least one vortex can pass through the film after appearance of the photon induced hot spot. This current is equal to I_{pass} when the vortex/antivortex pair is nucleated inside the hot spot or it is equal to I_{en} when the single vortex enters the hot spot via edge of the film. For the hot spot located at the edge of the film (see Fig. 2(a)) we also take into account that the vortex passes the film at current a bit larger than I_{en} .

IV. DEPENDENCE OF I_{det} ON THE LOCATION OF THE HOT SPOT AT $H=0$

In Fig. 4 we present dependence of I_{det} on the coordinate of center of HS with different radiuses $R = 2\xi$, 4ξ and 5ξ which roughly correspond to the photons with $\lambda/\eta = 25\mu m$, $6.3\mu m$ and $4.0\mu m$, respectively (note, that $\eta \simeq 0.1 - 0.4$ according to previous estimations [6, 16]

and for calculation of λ with help of Eq. (5) we use parameters of TaN film [16] with thickness $d = 3.9\text{nm}$. One can see that the minimum of the detection current is reached when HS 'touches' the edge of the film and it is maximal when HS seats in the center of the film. We argue that this result is the consequence of different current crowding at different locations of the hot spot in the film. Indeed, when HS approaches the edge of the film the current crowding increases in the narrowest sidewalk (and simultaneously the supervelocity inside the hot spot increases) and the vortices nucleate and becomes unpinned at the smaller applied current. But when the hot spot approaches the edge of the film its linear size decreases from $2R$ up to $\sqrt{2}R$ (we keep the area of the hot spot constant, because it is created by the photons of the same energy) and the current crowding decreases. It leads to increasing the applied current at which the vortex can enter the hot spot.

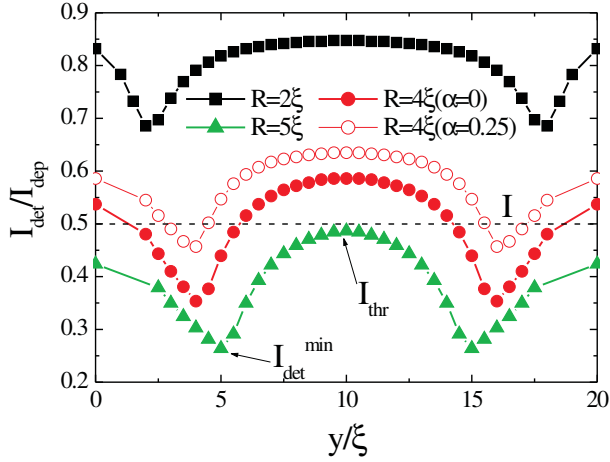


FIG. 4: Dependence of the detection current on the location of the hot spot with different radii in the film with $w = 20\xi$

How the results shown in Fig. 4 are related to the intrinsic detection efficiency of superconducting single photon detectors? Consider for example the photon which creates the hot spot with radius $R = 4\xi$. Let the transport current I is equal to $0.5I_{dep}$ (dashed line in Fig. 4). Then the part of the film where $I_{det} < I$ detects the absorbed photons while the rest of the film (regions near both edges and the center of the film) cannot detect such a photons and $IDE < 1$. Only when the current exceeds the threshold value ($I_{thr} = I_{det}^{max} \simeq 0.58I_{dep}$ for $R = 4\xi$) the whole film participates in detection of photons and $IDE = 1$.

If the transport current $I < I_{det}^{min} \simeq 0.35I_{dep}$ then IDE goes to zero in absence of fluctuations (when $R = 4\xi$). Fluctuations favor the creation of the vortices and they may provide the finite IDE even at $I < I_{det}^{min}$. To distin-

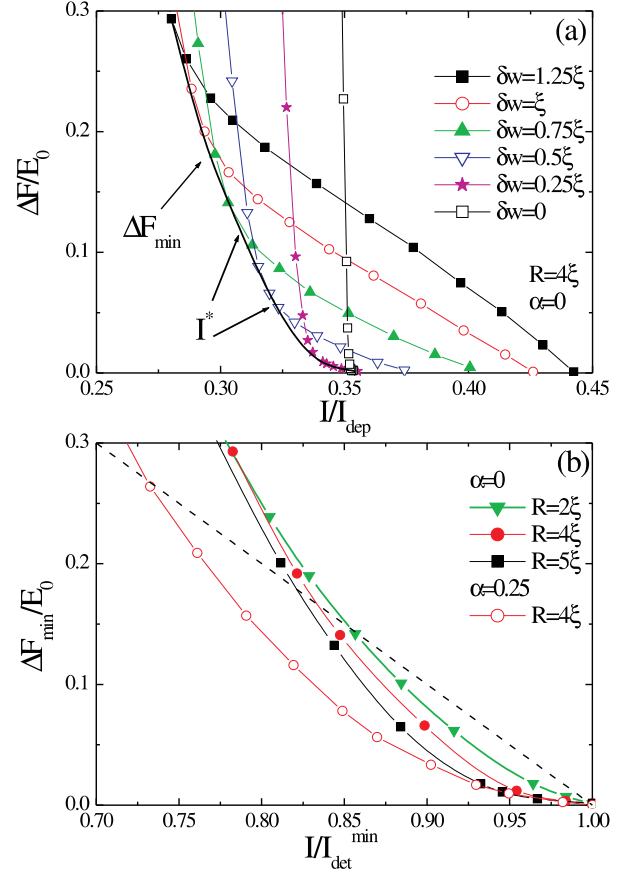


FIG. 5: (a) Energy barrier for the vortex entry to the hot spot with radius $R = 4\xi$ ($\alpha = 0$) located at different distances δw from the edge of the film. Solid line shows the minimal energy barrier at given value of the current. (b) Current dependence of the minimal barrier for the vortex entry to the hot spots with different radii and α . Dashed line corresponds to the dependence $\Delta F/E_0 = 1 - I/I_c$ following from the London model for the vortex entry to the straight film without the hot spot (when $I \sim I_c$).

guish this process from the current induced vortex penetration at the current $I > I_{en}$ we use the term 'fluctuation induced vortex penetration' when $I < I_{en}$. Because the barrier for the vortex entry increases rapidly with decreasing current [17–19] the main contribution to the fluctuation assisted IDE $\neq 0$ comes from the photons which create the hot spot near the edge of the film, where I_{det} is minimal. For this location of HS the vortex enters via the edge of the film and one needs to calculate the energy barrier for the vortex entry to the hot spot at $I < I_{en} = I_{det}$. In the Fig. 5(a) we show calculated barrier ΔF (the energy is scaled in units of $E_0 = \Phi_0^2 d / 16\pi^2 \lambda_L^2$) for the different locations of the hot spot with $R = 4\xi$ (ΔF is found using the numerical procedure from Ref. [19]). The energy barrier increases rapidly below some current $I^*(\delta w) < I_{det}(\delta w)$ (see Fig. 5(a)) because at currents $I \lesssim I^*$ the vortex cannot be pinned by the hot spot and it exits via the nearest edge of the film.

One can see from the Fig. 5(a) that for given value of the current there is a minimal barrier for the vortex entry ΔF_{min} when the hot spot is located at specific distance from the edge of the film. In Fig. 5(b) we show dependence $\Delta F_{min}(I)$ found for different radiuses of HS and α . Note that when $I \sim I_{det}^{min}$ the energy barrier increases much slowly with the current decrease as compared to the dependence $\Delta F(I)$ for the vortex entry to the film without HS, which follows from the London model [17, 18] ($\Delta F_L/E_0 \sim (1 - I/I_{dep})$ - see dashed line in Fig. 5(b)) or Ginzburg-Landau model [19] ($\Delta F_{GL}/E_0 \sim A(w)(1 - I/I_{dep})$, with $A(w) \sim 1.5 - 1.8$ for films with $w = 7 - 30\xi$) models at $I \sim I_{dep}$. Physically it is connected with suppressed order parameter in the sidewalk between the hot spot and edge of the film (see Fig. 3(a)). As a result it costs less energy for creation of the vortex (or vortex nucleus [19]) there.

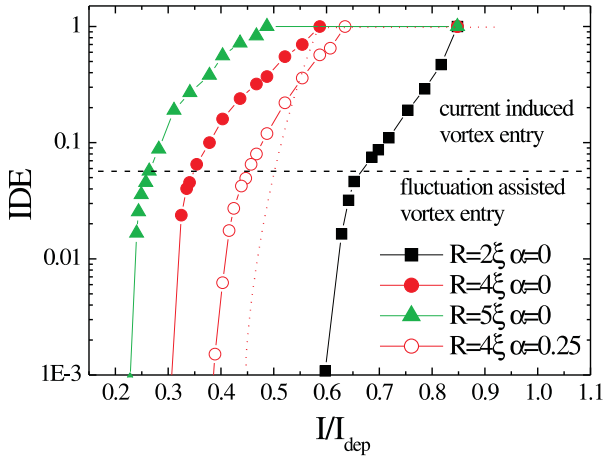


FIG. 6: Dependence of intrinsic detection efficiency on applied current which follows from nonmonotonic dependence $I_{det}(y)$ (at $I > I_{det}^{min}$) and finite probability for vortex entry due to fluctuations at $I < I_{det}^{min}$ (area below the dashed line). Dotted curve corresponds to dependence $IDE(I)$ following from the hot belt model [18] for one energy of the photon (qualitative presentation).

IDE in the fluctuation region could be found with help of Arrhenius law $IDE = \beta \exp(-\Delta F_{min}/k_B T)$ where the coefficient β in front of the exponent is equal IDE at $I \simeq I_{det}^{min}$ (we choose $\beta = 0.05$ because of rapid decrease of I_{det} near the I_{det}^{min} - see Fig. 4). Using parameters of TaN film [16] ($\lambda_L = 560nm$, $d = 3.9nm$) and $T = 4K$ we find $F_0/k_B T \simeq 62$. In Fig. 6 we plot IDE as a function of the current for photons with different wavelengths (which create the hot spots with different radiuses). In the same figure we plot the sketch of dependence $IDE(I)$ which follows from the hot belt model [18] (dotted curve). In the hot belt model $IDE < 1$ is explained exclusively by the effect of fluctuations, which leads to the fast drop of IDE with current decrease. Much smoother change of IDE from 1 up to $\simeq 0.05$ in the modified hot spot model exists even at $T = 0$ and it changes on much faster decay when $IDE \lesssim 0.05$ where it is finite only due to fluctuations

(qualitatively it is similar to the hot belt model).

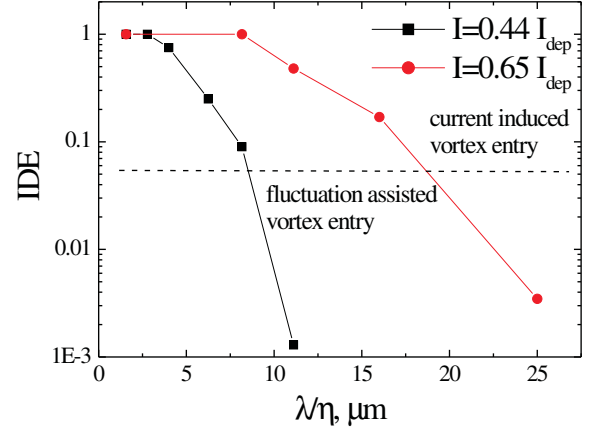


FIG. 7: Dependence of intrinsic detection efficiency on the wavelength for the superconducting film with $w = 20\xi$ and different transport currents. In calculations we use parameters of TaN film from Ref. [16].

We also calculate dependence $IDE(\lambda)$ at fixed current. For this purpose one needs to find the part of the film where $I_{det}(y)$ is smaller than the transport current for chosen R (i.e. wavelength). Because we know the barrier for the vortex entry to the hot spot we are able to calculate fluctuation induced IDE too. In Fig. 7 we present results of these calculations. As in dependence $IDE(I)$ one may distinguish two regions: relatively smooth variation of IDE with λ when it varies in the range $\sim 0.05 - 1$ and much faster decay of IDE at larger wavelengths, where IDE is finite only due to fluctuation assisted vortex entry to the hot spot. Qualitatively found results resemble experimentally observed dependence $IDE(\lambda)$ (see for example Refs. [3, 16]).

V. EFFECT OF THE MAGNETIC FIELD

How do dependencies $I_{det}(y)$ and $IDE(I)$ change in the presence of the applied magnetic field? In Fig. 8 we plot the current density distribution in the superconducting film with and without perpendicular magnetic field when there is no hot spot. One can see that in the presence of low magnetic field the current density increases in the left half of the film and it decreases in the right half of the film (for opposite direction of H the situation is opposite). Here under low magnetic field we mean fields $H < H_s/2$, where $H_s \simeq \Phi_0/4\pi\xi w$ is a magnetic field at which the surface barrier for vortex entry to the straight superconducting film is suppressed [20] (for film with $w = 20\xi$, $H_s/2 \simeq 0.025H_{c2}$). Using the results of section IV one may expect that the detection current becomes smaller (in comparison with the case $H = 0$) for HS appearing

in the part of the film with locally enhanced current density and vice versa in the opposite case. Our numerical calculations support this idea (see Fig. 9). Indeed, when H increases I_{det} decreases in the left half of the film and it increases in the right half of the film. Note that I_{det} changes much weaker in the central part of the film because of relatively small change of the current density there (see Fig. 8).

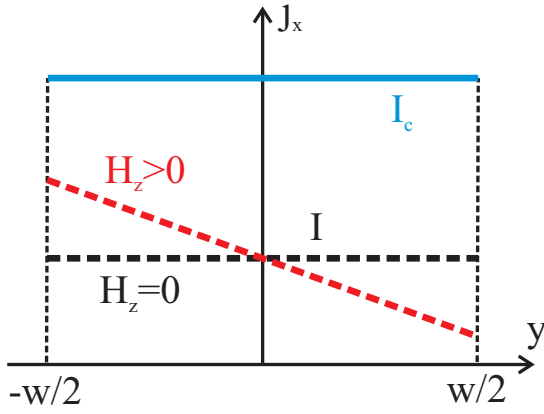


FIG. 8: Distribution of the current density in the narrow superconducting film with the transport current, placed in perpendicular magnetic field.

We also calculate the minimal energy barrier for the vortex entry (see Fig. 10) to the hot spot located near the left and right edges of the film at different magnetic fields. From Fig. 10 it follows that the shape of dependence $\Delta F_{min}(I)$ weakly changes at low magnetic fields $H \ll H_s$ while detection current in the left and right minima ($I_{det}^{L,R}$) varies linearly with the magnetic field (see inset in Fig. 10).

With the help of found results we calculate how IDE changes at weak magnetic fields (see Fig. 11). Because I_{thr} stays practically unchanged (see Fig. 9) while I_{det}^{min} decreases with increase of H (see inset in Fig. 10), the strongest change of IDE occurs at $I < I_{det}^{min}$ when $IDE \lesssim 0.05$. Note that the hot belt model [18] predicts relatively large change of IDE in whole range of $0 < IDE < 1$ and linear decrease of the threshold current when H increases (see dash-dotted curves in Fig. 11). Indeed, in the hot belt model I_{thr} is equal to the critical current of the film with the hot belt, which decreases linearly at weak magnetic field (like as I_{det}^L in the inset in Fig. 10).

VI. DISCUSSION

The vortex-assisted mechanism of the photon detection was discussed previously in several works [2, 3, 18, 21]. In contrast with Refs. [3, 21] we argue that the vortices play important role in all range of $0 < IDE < 1$ and not only when $IDE \ll 1$ is determined by the fluctuation assisted vortex entry or unbinding of the vortex-antivortex pair.

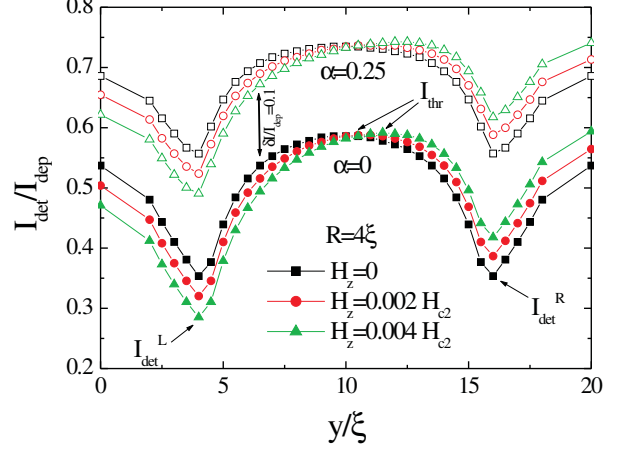


FIG. 9: Dependence of the detection current on the coordinate of the hot spot with $R = 4\xi$ (and $\alpha = 0, 0.25$) at different magnetic fields. Data for the hot spot with $\alpha = 0.25$ are shifted upwards by $\delta I / I_{dep} = 0.1$ for clarity.

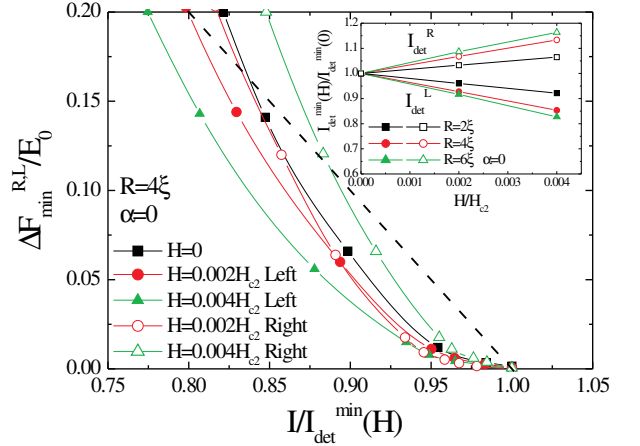


FIG. 10: Dependence of the minimal energy barrier for the vortex/antivortex entry to the hot spot located near the left/right edge of the film at different magnetic fields. Dashed line: $\Delta F_{min}/E_0 = 1 - I/I_{det}^{min}(H)$. In the inset we show dependence of $I_{det}^{L,R}(H)$ at low magnetic fields.

From the hot belt model [18] it follows that threshold current I_{thr} (at which IDE is about of unity) *decreases* linearly with increase of the magnetic field while we predict very weak dependence (increase) of I_{thr} at low magnetic fields $H \lesssim H_s \simeq \Phi_0 / 4\pi\xi w$.

Our model also predicts that at current $I \gtrsim I_{det}^{min}$ (where I_{det}^{min} depends on the radius of the hot spot and, hence, on the energy of the photon - see Fig. 4) the

photon count rate varies with the magnetic field much weaker than at smaller currents (see Fig. 11 - note, that some signs of this effect were observed in Ref. [25] - see Fig. 3 there). To observe this effect experimentally it is preferable to use the materials with the threshold current I_{thr} much smaller than critical current of the superconducting film (like in materials studied in Refs. [16, 22–24]) because in this case one can vary magnetic field in wide range and do not overcome the critical current $I_c(H)$. Experimentally I_{det}^{min} for each photon's wavelength could be determined from the dependence of detection efficiency (DE) on the current if it saturates (and $DE(I)$ has a plateau) at large currents. According to our calculations at $I = I_{det}^{min}$ the $DE \simeq 0.05 DE_{plateau}$ (which corresponds to $IDE \simeq 0.05$). But in our model we consider only straight homogenous film, while real SSPD are based on the superconducting meanders which have the bends, structural defects and variations of the thickness and/or width. Therefore the minimal detection current may correspond to the different location of the hot spot when the found for the straight film. To demonstrate this effect in Fig. 12 we show calculated dependence $I_{det}(y)$ for the film with 90° degree bend (see inset in Fig. 12). From Fig. 12 one can see that the photon absorbed near the inner corner of the bend (the current density is maximal there due to current crowding) could be detected at the smallest transport current. From comparison of Fig. 12 with Fig. 9 one can also see that the bend acts like a weak magnetic field. This similarity is not accident because in both cases there are places in the film where the local current density is maximal and the minimal detection current corresponds to the absorption of the photon near that places.

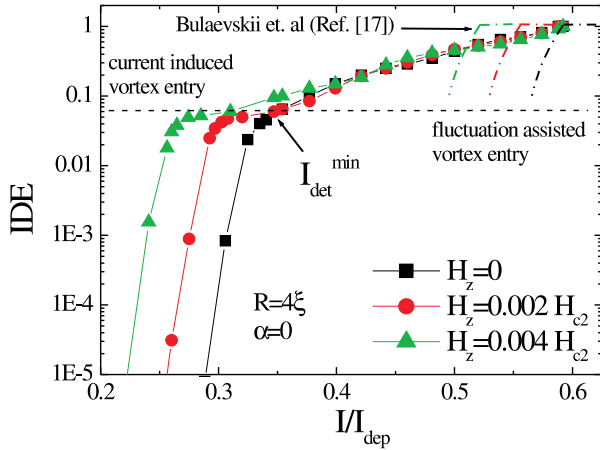


FIG. 11: Dependence of the intrinsic detection efficiency on the current at different magnetic fields. Dashed-dotted lines correspond to the dependences $IDE(I)$ following from the hot belt model at different magnetic fields [18] (qualitative presentation).

This result demonstrates that in the bent *homogenous* film the area near the bend determines both I_{det}^{min} and minimal IDE, which is not connected with the fluctua-

tion assisted vortex entry. For example, at $I = 0.28 I_{dep}$ (which is a little above the minimal detection current for the hot spot with $R = 4\xi$ located near the bend - see Fig. 12) the minimal energy barrier for the vortex entry to the straight part of the film with the hot spot is about $0.29 E_0$ (see Fig. 5(a)). Taking into account that typically $E_0/k_B T \gtrsim 50$ one easily find that the vortex penetration to the straight part of the film is suppressed by factor $\exp(-\Delta F/k_B T) \lesssim 10^{-6}$ which is much smaller than the ratio between the area near the bends and the rest of the superconducting meander (which is about $10^{-2} - 10^{-3}$ depending on how to estimate the 'active' area near the bend). Therefore we expect that in real SSPD the fluctuation assisted vortex entry contributes to the finite IDE when it becomes smaller than $\lesssim 10^{-3} - 10^{-2}$.

The actual boundary between the fluctuation assisted and the current induced vortex penetration (leading to the detection of the photon) could be deduced from the experiment with the magnetic field. Indeed, because the first mechanism is more sensitive to the magnetic field (see Fig. 11) the IDE at currents $I < I_{det}^{min}$ should increase much faster than at larger currents.

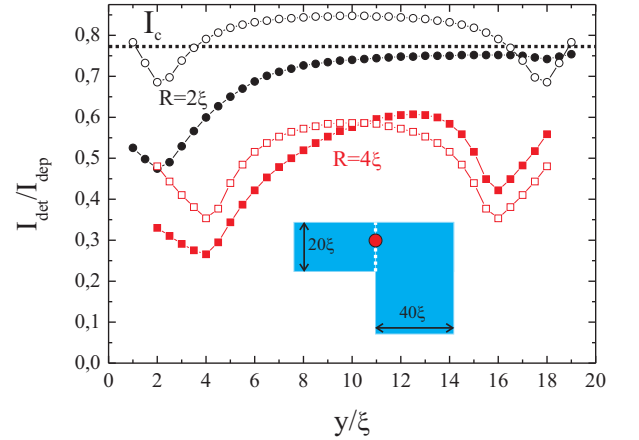


FIG. 12: Dependence of the detection current on the coordinate of the hot spot with radius $R = 2\xi$ (solid circles) and $R = 4\xi$ (solid squares) along the white line in the bent film shown in the inset. In the same figure we show I_{det} for the straight film with $w = 20\xi$ (empty circles and squares). The critical current of the film with the bend $I_c = 0.77 I_{dep}$ (dotted line).

Discussed above effect could explain the absence of dependence of the photon count rate (PCR) on the magnetic field, experimentally found in Ref. [26]. Indeed, in that work the field dependence was studied in the current interval where PCR was changed from its maximal value by two orders of magnitude (which is equivalent to similar change in IDE). Therefore it might be that the minimal used current still was larger than I_{det}^{min} . As a result at used in Ref. [26] magnetic fields $H < 100 Oe$ and

$H_s \sim 4000 Oe$ (it is called as H^* in Ref. [26]) the PCR could change not more than by several percents (following the change of I_{det}^{min} - see Fig. 9), which is about of the experimental error in Ref. [26].

On the contrary, in Ref. [25] the strong dependence of PCR on magnetic field was found at low currents. Comparison of the obtained results with the predictions of the hot belt model [18] made in Ref. [25] demonstrated good qualitative but bad quantitative agreement. To fit the experimental results authors needed special dependence of the characteristic vortex energy (in the presence of the hot belt - see Eq. (3) in Ref. [25]) on the wavelength and current (see insets in Fig. 2(b) and 3 in Ref. [25]) which does not follow from the theory of Ref. [18]. Our model also predicts the strong dependence of PCR on the magnetic field, but only at the current $I < I_{det}^{min}(\lambda)$. Because the current dependence of the energy barrier for the vortex entry is not linear (see Figs. 5(b),10) we expect quasi-exponential increase of PCR at low magnetic fields which differs from the exponential law (see for example Eq. (2) in [25] or Eq. (5) in [26]) following from the linear dependence $\Delta F(I)$ in the London model. To make the quantitative comparison with Ref. [25] one needs to calculate the IDE(I) for the film with the bends (using the same procedure as in the present work for the straight film) and find the energy barrier for the vortex entry to the hot spot, located close to the bend. Our present results give only qualitative prediction that there exist some current I_{det}^{min} (at this current $IDE \sim 10^{-3} - 10^{-2}$) above which the photon count rate weakly depends on H and at smaller currents it depends on weak magnetic fields much stronger (quasi-exponentially).

VII. CONCLUSION

In the framework of the modified hot spot model we predict that the intrinsic detection efficiency of supercon-

ducting single photon detector gradually changes with the current. The change of IDE from 1 to ~ 0.01 occurs due to dependence of the current, at which the resistive response appears, on the location of the hot spot in the film. The resistive state starts from the vortex entry (when the hot spot is located near or at the edge of the film) or nucleation of the vortex-antivortex pair (when hot spot is located far from the edge) and their motion across the film. The change of IDE from ~ 0.01 up to zero is connected with the fluctuation assisted vortex entry to the hot spot located near the edge of the film, when the current itself cannot cause the vortex entry.

Weak applied magnetic field ($H \ll \Phi_0/4\pi\xi w$ strongly affects (increases) $IDE \ll 1$ when it is nonzero only due to fluctuation assisted vortex entry to the hot spot. At the currents close to the threshold current, at which $IDE \simeq 1$, the applied magnetic field weakly affects the detection ability and may provide only increase of I_{thr} .

Acknowledgments

We thank to Alexander Semenov, Gregory Gol'tsman, Alexey Semenov, Jelmer Renema, Michiel de Dood and Martin van Exter for valuable discussion of the found results. The work was partially supported by the Russian Foundation for Basic Research (project 12-02-00509) and by the Ministry of education and science of the Russian Federation (the agreement of August 27, 2013, N 02.49.21.0003 between The Ministry of education and science of the Russian Federation and Lobachevsky State University of Nizhni Novgorod).

-
- [1] R. Lusche, A. Semenov, H. Huebers, K. Ilin, M. Siegel, Y. Korneeva, A. Trifonov, A. Korneev, G. Goltsman, and D. Vodolazov, arXiv:1303.4546.
 - [2] A. Zotova and D. Y. Vodolazov, Phys. Rev. B **85**, 024509 (2012).
 - [3] M. Hofherr, D. Rall, K. Il'in, M. Siegel, A. Semenov, H.-W. Hübers, and N. A. Gippius, J. of Appl. Phys. **108**, 014507 (2010).
 - [4] A. D. Semenov, G. N. Gol'tsman, and A. A. Korneev, Phys. C (Amsterdam) **351**, 349 (2001).
 - [5] L. Maingault, M. Tarkhov, I. Florya, A. Semenov, R. Espiau de Lamaëstre, P. Cavalier, G. Goltsman, J.-P. Poizat, and J.-C. Villégier, J. Appl. Phys. **107**, 116103 (2010).
 - [6] A. Semenov, A. Engel, H.-W. Hübers, K. Il'in, and M. Siegel, Eur. Phys. J. B **47**, 495 (2005).
 - [7] A. Engel and A. Schilling, J. Appl. Phys. **114**, 214501 (2013).
 - [8] J. R. Clem and K. K. Berggren, Phys. Rev. B **84**, 174510 (2011).
 - [9] J. R. Clem, Y. Mawatari, G.R. Berdiyrov and F.M. Peeters, Phys. Rev. B **85**, 144511 (2012).
 - [10] D. Henrich, P. Reichensperger, M. Hofherr, K. Il'in, M. Siegel, A. Semenov, A. Zotova and D. Yu. Vodolazov, Phys. Rev. B **86**, 144504 (2012).
 - [11] H. L. Hortensius, E. F. C. Driessen, T. M. Klapwijk, K. K. Berggren and J. R. Clem, Appl. Phys. Lett. **100**, 182602 (2012).
 - [12] M. K. Akhlaghi, H. Atikian, A. Eftekharian, M. Loncar, A. H. Majedi, Optics Express, **20**, 23610 (2012).
 - [13] O.-A. Adami, D. Cerbu, D. Cabosari, M. Motta, J. Cuppens, W.A. Ortiz, V.V. Moshchalkov, B. Hackens, R. Delamare, J. Van de Vondel, A.V. Silhanek, Appl. Phys. Lett. **102**, 052603, 2013.
 - [14] A. G. Kozorezov, A. F. Volkov, J. K. Wigmore, A. Peacock, A. Poelaert, and R. den Hartog, Phys. Rev. B **61**,

- 11 807 (2000).
- [15] D.Y. Vodolazov, I.L. Maksimov, E.H. Brandt, *Physica C* **384**, 211 (2003).
 - [16] A. Engel, A. Aeschbacher, K. Inderbitzin, A. Schilling, K. Il'in, M. Hofherr, M. Siegel, A. Semenov, and H.-W. Hübbers, *Appl. Phys. Lett.* **100**, 062601 (2012).
 - [17] H. Bartolf, A. Engel, A. Schilling, K. Il'in, M. Siegel, H.-W. Hübbers and A. Semenov, *Phys. Rev. B* **81**, 024502 (2010).
 - [18] L. N. Bulaevskii, M. J. Graf, and V. G. Kogan, *Phys. Rev. B* **85**, 014505 (2012).
 - [19] D. Y. Vodolazov, *Phys. Rev. B* **85**, 174507 (2012).
 - [20] G. Stejic, A. Gurevich, E. Kadyrov, D. Christen, R. Joynt, and D.C. Larbalestier, *Phys. Rev. B* **49**, 1274 (1994).
 - [21] A. D. Semenov, P. Haas, H.-W. Hübbers, Konstantin Il'in, M. Siegel, A. Kirste, T. Schurig, A. Engel, *Physica C* **468** 627 (2008).
 - [22] F. Marsili, V. B. Verma, J. A. Stern, S. Harrington, A. E. Lita, T. Gerrits, I. Vayshenker, B. Baek, M. D. Shaw, R. P. Mirin, and S. W. Nam, *Nature Photonics*, **7**, 210, 2013.
 - [23] Y. P. Korneeva, M. Y. Mikhailov, Y. P. Pershin, N. N. Manova, A. V. Divochiy, Y. B. Vakhtomin, A. A. Korneev, K. V. Smirnov, A. Y. Devizenko, and G. N. Goltsman, arXiv:1309.7074 [cond-mat.supr-con].
 - [24] V. B. Verma, A. E. Lita, M. R. Vissers, F. Marsili, D. P. Pappas, R. P. Mirin, and S. W. Nam, arXiv:1402.4526 [cond-mat.supr-con].
 - [25] R. Lusche, A. Semenov, Y. Korneeva, A. Trifonov, A. Korneev, G. Gol'tsman, and H.-W. Hübbers, *Phys. Rev. B* **89**, 104513 (2014).
 - [26] A. Engel, A. Schilling, K. Il'in and M. Siegel, *Phys. Rev. B* **86**, 140506(R) (2012).